

**Tristability in the pendula chain**Ramaz Khomeriki<sup>1,2</sup> and Jérôme Leon<sup>3</sup><sup>1</sup>*Physics Department, Tbilisi State University, 0128 Tbilisi, Georgia*<sup>2</sup>*Max-Planck-Institut für Physik komplexer Systeme, 01187 Dresden, Germany*<sup>3</sup>*Laboratoire de Physique Théorique et Astroparticules, CNRS-IN2P3 (UMR 5207), Université Montpellier 2, 34095 Montpellier, France*

(Received 10 May 2008; published 12 November 2008)

Experiments on a chain of coupled pendula driven periodically at one end demonstrate the existence of a regime which produces an output frequency at an odd fraction of the driving frequency. The stationary state is then obtained with numerical simulations and modeled with an analytical solution of the continuous sine-Gordon equation that resembles a kinklike motion back and forth in the restricted geometry of the chain. This solution differs from the expressions used to understand nonlinear bistability where the synchronization constraint was the basic assumption. As a result the short pendula chain is shown to possess tristable stationary states and to act as a frequency divider.

DOI: [10.1103/PhysRevE.78.057202](https://doi.org/10.1103/PhysRevE.78.057202)

PACS number(s): 05.45.-a, 73.43.Lp

**I. INTRODUCTION**

The sine-Gordon model and its discrete analog, the Frenkel-Kontorova chain, are among the most prominent equations of nonlinear physics, and have attracted interest of people working in quite different fields, see, e.g., Refs. [1–3]. In particular, topological (kinks) and nontopological (breathers) solutions of the sine-Gordon equation describe the dynamics of nonlinear excitations in various spatially modulated systems, e.g., dislocations in crystals [4], magnetic and ferroelectric domain walls' motion [5], vortices in arrays of Josephson junctions [6], etc. At the same time the model has a simple experimental counterpart, namely, the chain of linearly coupled pendula [3] which offers an interesting opportunity to easily visualize all the main nonlinear characteristics of the sine-Gordon system. Then this simple laboratory tool allows one to observe effects [7–10] which may then apply in completely different physical situations.

As a matter of fact, a recent experimental discovery of the supratransmission effect in the pendula chain [11] has led to the study of similar phenomena in optical Bragg gratings [12], Josephson junction transmission line [13], and waveguide arrays [14,15]. By this approach, many similar phenomena observed in the same systems [16–20] have been identified as effects of nonlinear bistability. Moreover it allowed us to predict the existence of bistable magnetization profiles in thin magnetic films [21] and to suggest ultrasensitive detectors (or digital amplifiers) in optical waveguides [22], quantum Hall bilayers [23], and Josephson Junction parallel arrays [24].

The bistability property can be simply formulated by saying that [25] a given periodic boundary driving may produce two completely different stationary states: One which tends to the linear evanescent profile at vanishing amplitude, and the other one which can be qualitatively understood as a portion of the stationary breather like solution which exists only if the system size is comparable with the characteristic length of the fundamental (continuous) breather solution. This is a main difference with most of the earlier studies on the sine-Gordon model where the semi-infinite chain has been examined (see, e.g., Ref. [26]).

We report here the discovery of a third stationary state which can be qualitatively understood as the motion back and forth of a kinklike structure in the short pendula chain. The stationary regime appears to be completely different from the two cases considered earlier, e.g., in Refs. [21–25]. As a matter of fact, such a dynamics creates a frequency in the system and furnishes a tool to divide the input frequency by odd fractions (we shall illustrate chain end oscillations with frequency  $\Omega/3$  or  $\Omega/5$ , where  $\Omega$  is the driver frequency). The value of the odd divider depends both on the input frequency range and on the length of the chain. Let us recall that the previously discovered two regimes are synchronized to the driver (same input and output frequencies).

**II. MODEL EQUATIONS**

The dynamics of the chain of  $N$  pendula is naturally described by the Frenkel-Kontorova model [1]

$$\ddot{u}_n + \delta \dot{u}_n - \sigma^2(u_{n+1} + u_{n-1} - 2u_n) + \omega_0^2 \sin u_n = 0, \quad (1)$$

where an overdot means derivation with respect to time. The variable  $u_n$  is the angular deviation of the  $n$ th pendulum,  $\omega_0$  is the eigenfrequency of a single pendulum, and  $\sigma$  is proportional to the linear torsion constant of the spring (for our experimental chain  $\omega_0 = 15.1$  Hz,  $\sigma = 32.4$  Hz). The damping coefficient  $\delta$  is phenomenological; it has been evaluated in the experiments as approximately  $\delta = 0.01\omega_0$ . This is the value actually used in the numerical simulations. The applied periodic driving is here modeled by the boundary conditions

$$u_0(t) = b \cos(\Omega t), \quad u_{N+1} = u_N \quad (2)$$

which model a forced end in  $n=0$  and a free other end in  $n=N$ .

It is worth insisting on the fact that the chain is submitted to a prescribed boundary value [the datum of  $u_0(t)$ ], not to a given force acting on the first particle. In the experimental setup, the motion of the virtual pendulum  $u_0$  is the driving engine motion which has indeed a prescribed motion obtained through feedback control. This has an important fun-

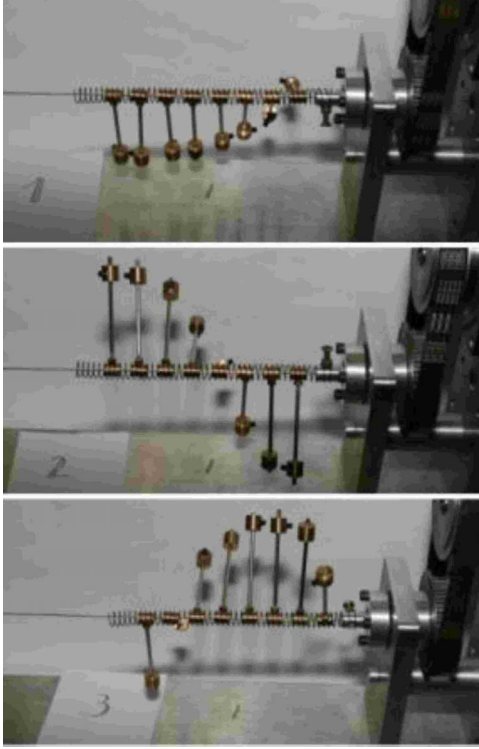


FIG. 1. (Color online) Pictures of three stationary states of the pendula chain obtained for one single given driving amplitude and frequency. The upper graph corresponds to the lowest energy state and the lower one describes the largest energy regime. An approximate energy hierarchy is 1:10:100.

damental consequence: the energy absorbed by damping is continuously compensated by the action of the driving and therefore the motion of the chain is quite similar to that of an undamped device (for which, in a stationary regime, the driving would not give energy to the chain).

The experiment consists thus in driving the short chain pictured in Fig. 1 with a frequency in the forbidden band gap ( $\Omega < \omega_0$ ), which actually does not excite linear modes. Without external perturbation the system locks to a periodic solution with low output amplitude  $u_N(t)$ . Depending on the value of an external kick one makes the system bifurcate to two different stationary states and we thus obtain a tristable behavior (with approximate hierarchy of energies 1:10:100). The reader will find in Ref. [27] a movie of the experiment where the system is first set in the high-energy new stationary stable regime and then put down successively to the two others stable states by taking energy off.

To develop an analytical description of the process, let us consider the continuous approximation of Eq. (1) by substitutions  $t \rightarrow \omega_0 t$ ,  $n = \omega_0 x / \sigma$ . Neglecting dissipation we obtain the sine-Gordon equation

$$x \in [0, L] : u_{tt} - u_{xx} + \sin u = 0, \quad (3)$$

where  $L = N\sigma / \omega_0$ . The mixed Dirichlet and Neumann boundary conditions  $u(0, t) = b \sin(\Omega t)$  (driven boundary),  $u_x(L, t) = 0$  (free end boundary) allows us to seek the following periodic stationary solutions [25]:

$$u(x, t) = 4 \arctan \left[ \sqrt{\frac{rs}{b}} \left[ \mathcal{X}(x) \mathcal{T}(t) \right] \right], \quad (4)$$

where one has three choices (cn, sn, and dn are the standard Jacobi elliptic functions)

$$(I) \mathcal{X} = \text{cn}[\beta(x-L), \mu], \quad \mathcal{T} = \text{cn}(\omega t, \nu),$$

$$(II) \mathcal{X} = \text{dn}[\beta(x-L), \mu], \quad \mathcal{T} = \text{sn}(\omega t, \nu),$$

$$(III) \mathcal{X} = \text{dn}[\beta(x-L) + \mathbb{K}(\mu), \mu], \quad \mathcal{T} = \text{sn}(\omega t, \nu). \quad (5)$$

Here  $\mathbb{K}(\mu)$  stands for a complete elliptic integral of the first kind of modulus  $\mu$ . These families of solutions are parametrized by the two free constants  $\omega$  and  $\nu \in [0, 1]$ ; then for solutions of type I the remaining parameters are given by

$$\begin{aligned} b &= \omega^4 \nu^2 (1 - \nu^2), \quad s = \omega^2 \nu^2, \\ 2r &= 1 - \omega^2 + 2\omega^2 \nu^2 + \sqrt{(1 - \omega^2)^2 + 4\omega^2 \nu^2}, \\ \beta^2 &= \frac{b + r^2}{r}, \quad \mu^2 = \frac{r^2}{b + r^2}, \end{aligned} \quad (6)$$

while in both cases II and III they read

$$\begin{aligned} b &= \omega^4 \nu^2, \quad s = -\omega^2 \nu^2, \\ 2r &= 1 - \omega^2 (1 + \nu^2) + \sqrt{[1 - \omega^2 (1 + \nu^2)]^2 - 4\omega^4 \nu^2}, \\ \beta^2 &= r, \quad \mu^2 = 1 - \frac{b}{r^2}. \end{aligned} \quad (7)$$

Note that  $r$  should be real valued and positive which may restrict the allowed values of  $\omega$ .

### III. TRISTABILITY AND FREQUENCY DIVISION

Since the experiments (confirmed by numerical simulations later on) show that the frequency  $\Omega/3$  can also be excited, we assume that the period of the time dependent part  $\mathcal{T}(t)$  of the stationary solutions (5) coincide with an odd integer fraction of the driving frequency  $\Omega$ . Recalling that the period of  $\mathcal{T}(t)$  is  $4\mathbb{K}(\nu)/\omega$  we require thus

$$\omega = 2\Omega \mathbb{K}(\nu) / (m\pi), \quad (8)$$

where  $m$  is an odd integer. For a given value of the parameter  $\nu \in [0, 1]$ , the above relation fixes the second parameter  $\omega$  in terms of the driving frequency  $\Omega$ . Therefore fixing  $\Omega$  (driver frequency) and varying  $\nu$  one can plot the output amplitude  $u(N, t)$  in terms of the input  $u(0, t)$  from the analytic expressions (5). We display this dependence for  $\Omega = 0.9$  (in units of  $\omega_0$ ) as a full line in Fig. 2 where different colors report to different solutions. We also plot (dashed line) the output amplitude for a driving frequency  $\Omega = 0.3$ . Therefore, to the given driver amplitude  $\max_t |u(0, t)| = 0.5$  may correspond to two stable synchronized states (points 1 and 2 on the graph) having the driver frequency 0.9 and one more stable state with frequency 0.3.

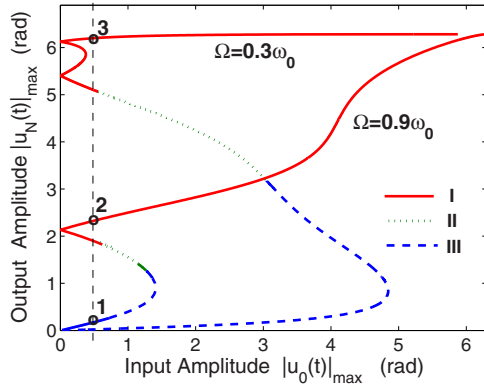


FIG. 2. (Color online) Analytic input-output amplitude dependences for different oscillation frequencies of stationary states given by formulas (5) where continuous line represents solution (I), dotted line solution (II), and dashed line solution (III), plotted for two frequencies, namely,  $0.9\omega_0$  and  $0.3\omega_0$  as indicated. The points 1, 2, and 3 correspond to the stable regimes with a single driving amplitude  $|u_0(t)|_{\max}=0.5$  rad. The points 1 and 2 represent the situations when the whole chain oscillates with the driving amplitude  $0.9\omega_0$  but with different output amplitudes. The point 3 corresponds to the driving frequency  $0.3\omega_0$  and describes kink motion forth and back. As the experiments and numerical simulations show (and this is a main finding of the paper), the latter regime can also be reached with a driving frequency  $0.9\omega_0$  three times larger than the one actually used.

It is then a simple matter to check that the stationary state related to point 3 of the plot of Fig. 2 corresponds effectively to our numerical simulations, and hence to the experiments of Fig. 1. It is done in Fig. 3, where the last plot shows the result of a numerical simulation (full line) compared with the analytic solution (dashed line) related to point 3 of Fig. 2. We have also plotted the time evolution of the total energy of each pendulum given by

$$E_n = \frac{1}{2} \dot{u}_n^2 + \frac{\sigma^2}{4} [(u_{n+1} - u_n)^2 + (u_{n-1} - u_n)^2] + \omega_0^2 (1 - \cos u_n). \tag{9}$$

The numerical simulations of the process are done by applying to the model (1) the boundary conditions (2) with  $b=0.5$  and  $\omega=0.9\omega_0$ , together with an initial condition where a few pendula at the end of the chain are given large initial amplitude. For instance, to reach the new stationary state (3) of Fig. 3, the chosen initial amplitude is  $2\pi$ , while for the value  $\pi$ , the system locks to the state (2).

It is worth noting that both experiments (as those displayed in Ref. [27]) and numerical simulations contain intrinsic damping. Still the analytic solutions of the continuous undamped sine-Gordon model fit strikingly well numerical simulations of the discrete damped Frenkel-Kontorova model (1). This is a general property of such short length driven systems to lock on fundamental solutions of the undamped limit, as previously displayed in Refs. [23,24,28]. The main fact is that, without damping, the chain in a stationary regime does not absorb energy and the boundary value does not transfer any power to the chain. With damp-

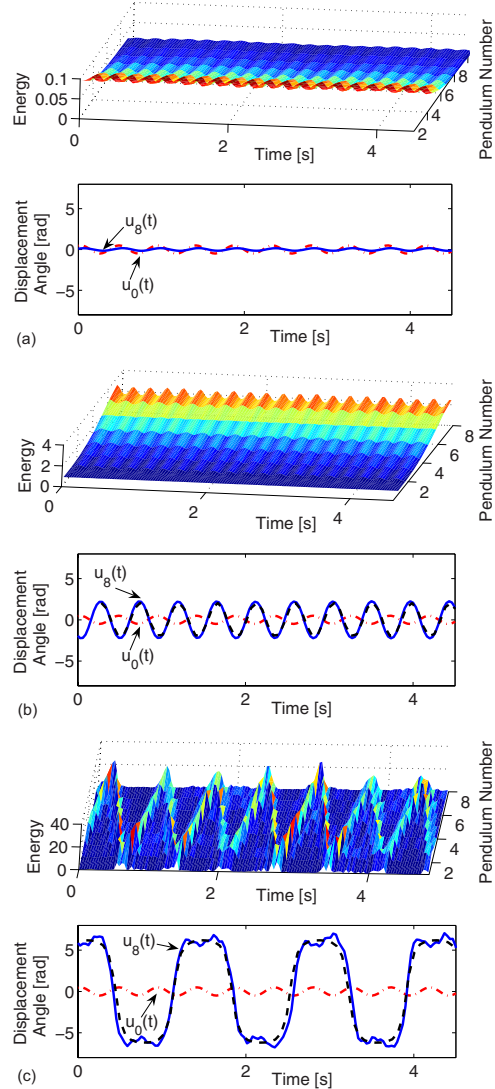


FIG. 3. (Color online) Numerical simulations on Frenkel-Kontorova model (1) with a damping constant  $\delta=0.01\omega_0$  and eight pendula. The time evolution of pendula energy and input-output oscillations are displayed corresponding to the points numbered 1, 2, and 3 in Fig. 2. The driving amplitude is  $|u_0(t)|_{\max}=0.5$  rad and its frequency  $\Omega=0.9\omega_0$  for all three cases. This results in the same output frequency oscillations  $\Omega$  in graphs (a) and (b) but  $\Omega/3$  output oscillations in graph (c). Dashed lines display analytical curves obtained from Eq. (5), while dotted-dashed and solid lines represent time evolution of input and output oscillations, respectively.

ing, the driving boundary does transmit power to the chain in such a way as to compensate exactly for the losses. The point is that the system is submitted to a prescribed boundary value which adapts to the amount of lost power and keeps amplitude and frequency constants (in the experiments presented in Fig. 1, the engine has a feedback driving mechanism that controls the amplitude and frequency). Last, the proof that the analytical solutions constitute an attractor for the damped system is, as far as we know, an open question.

Thus we have actually demonstrated the possibility of conceiving a frequency divider with which the driving frequency can be divided by 3, 5, or 7, depending on the chain

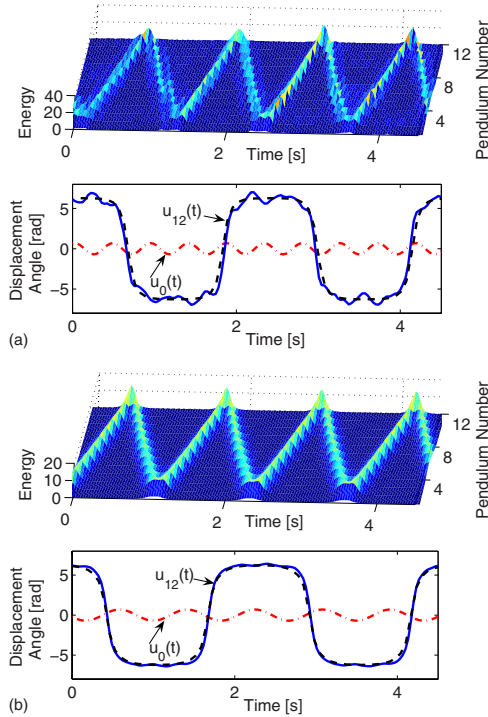


FIG. 4. (Color online) Time evolution of pendula energy and input-output oscillations for the chain consisting of 12 pendula. As seen one gets the frequency division on 5 at the output with respect to the input frequency when the input frequency is  $\Omega = 0.9\omega_0$  [graph (a)]. In graph (b) the driving frequency is  $\Omega = 0.5\omega_0$  and one has frequency division by factor 3.

length. For example, Fig. 4 shows numerical simulations on a chain of 12 pendula with a resulting frequency division by 5 at a driving frequency  $0.9\omega_0$  and by 3 at a driving frequency  $0.5\omega_0$ . In such a case we have obtained that the frequency is divided by 5 if the driving frequency  $\Omega$  is in the range  $0.88\omega_0 < \Omega < 0.92\omega_0$ , while the same chain can divide the frequency by 3 when  $0.41\omega_0 < \Omega < 0.6\omega_0$ .

#### IV. CONCLUSION

For a single monochromatic driving (fixed amplitude and frequency), we have demonstrated experimentally and numerically the existence of three states which have been given analytic expressions (in the continuous limit): the first one is the quasilinear solution (actually a breatherlike tail) and the second one resembles half a breather, both of them oscillating with the driving frequency  $\Omega$ , and which were already known as the building blocks of nonlinear bistability. The discovered third state resembles a kink moving back and forth with the frequency  $\Omega/3$ . These states have been given explicit analytical expressions in the continuous limit: the first state is described by the solution of type (III) in Eq. (5) while the solution of type (I) describes altogether the “half-breather” with frequency  $\Omega$  and the “oscillating kink” with frequency  $\Omega/3$ .

The process of frequency division is thus induced by the motion back and forth of a kinklike structure inside the chain. It is possible to extend these studies to other realistic physical systems governed by the sine-Gordon equation. We expect such a stationary stable regime to be interesting for applications where one is interested in producing an odd fraction of the driving frequency. The fraction number depends both on the length of the chain and on the input frequency range. Last but not least, many other well known nonlinear systems exhibit nonlinear bistable behavior, such as, e.g., the nonlinear Schrödinger equation or the coupled mode system in Bragg media, and this discovery is very likely to apply also there.

#### ACKNOWLEDGMENTS

We thank Dominique Chevriaux for the production of the movie on the pendula chain. R.K. acknowledges financial support of the Georgian National Science Foundation (Grant No. GNSF/STO7/4-197) and USA Civilian Research and Development Foundation (Grant No. GEP2-2848-TB-06).

- [1] O. M. Braun and Yu. S. Kivshar, *The Frenkel-Kontorova Model: Concepts, Methods, and Applications* (Springer-Verlag, Berlin, 2004).
- [2] M. Remoissenet, *Waves Called Solitons* (Springer, Berlin, 1999).
- [3] A. C. Scott, *Nonlinear Science*, 2nd ed. (Oxford University Press, New York, 2003).
- [4] M. El-Batanouny *et al.*, Phys. Rev. Lett. **58**, 2762 (1987).
- [5] Xin Liu *et al.*, Phys. Rev. B **71**, 224419 (2005).
- [6] J. Pfeiffer *et al.*, Phys. Rev. B **77**, 024511 (2008).
- [7] R. Chacon and P. J. Martinez, Phys. Rev. Lett. **98**, 224102 (2007).
- [8] N. V. Alexeeva *et al.*, Phys. Rev. Lett. **84**, 3053 (2000).
- [9] W. Chen *et al.*, Phys. Rev. B **65**, 134302 (2002).
- [10] Yu. A. Kosevich *et al.*, Phys. Rev. E **77**, 046603 (2008).
- [11] F. Geniet and J. Leon, Phys. Rev. Lett. **89**, 134102 (2002).
- [12] J. Leon and A. Spire, Phys. Lett. A **327**, 474 (2004).
- [13] F. Geniet and J. Leon, J. Phys.: Condens. Matter **15**, 2933 (2003).
- [14] J. Leon, Phys. Rev. E **70**, 056604 (2004).
- [15] R. Khomeriki, Phys. Rev. Lett. **92**, 063905 (2004).
- [16] H. G. Winful *et al.*, Appl. Phys. Lett. **35**, 379 (1979).
- [17] W. Chen and D. L. Mills, Phys. Rev. B **35**, 524 (1987).
- [18] O. H. Olsen and M. R. Samuelsen, Phys. Rev. B **34**, 3510 (1986).
- [19] D. Barday and M. Remoissenet, Phys. Rev. B **41**, 10387 (1990).
- [20] Y. S. Kivshar *et al.*, Phys. Lett. A **168**, 391 (1992).
- [21] R. Khomeriki *et al.*, Phys. Rev. B **74**, 094414 (2006).
- [22] R. Khomeriki and J. Leon, Phys. Rev. Lett. **94**, 243902 (2005).
- [23] R. Khomeriki *et al.*, Eur. Phys. J. B **49**, 213 (2006).
- [24] D. Chevriaux *et al.*, Phys. Rev. B **73**, 214516 (2006).
- [25] R. Khomeriki and J. Leon, Phys. Rev. E **71**, 056620 (2005).
- [26] M. D. Miller, Phys. Rev. B **33**, 1641 (1986).
- [27] <http://www.lpta.univ-montp2.fr/users/leon/Bistable/>.
- [28] K. Tse Ve Koon *et al.*, Phys. Rev. E **75**, 066604 (2007).